

D(*d,p*)T fusion induced by heavy-ion irradiation of TiD_{1.7}

T. W. Workman and M-A. Nicolet

California Institute of Technology, Pasadena, California 91125

(Received 8 June 1992)

As a test of the linear cascade model for ion-solid interaction, Xe and Ar ion irradiation at energies of 140–600 keV is used to induce D+D fusion in TiD_{1.7}. The fusion yield is measured by monitoring the 3.02-MeV protons from the D(*d,p*)T reaction. A linear binary-collision cascade model predicts fusion yields that are in excellent agreement with the measured yields for all cases studied.

The chain of events that occurs as an energetic ion penetrates a solid is of great interest to those studying ion implantation and ion mixing. When the collision cascade caused by an energetic ion results in atoms being ejected from the surface, the quantity, energy, and direction of these sputtered particles can be measured directly.¹ For example, Auger electron emission from sputtered atoms or atoms in the near surface region (the first 3 nm) can give information about the collision cascade close to the surface.^{2,3} However, the collision cascade deeper within a solid has so far never been directly observed due to the extremely short time scale and small distances involved. Experimental data giving indirect information about the collision cascade include concentration of defects, the spreading of an interface between two different atomic species (ion mixing), and ion range and straggling, all of which are measured after ion irradiation.

Another measurement that gives information about the collision cascade is nuclear reaction analysis. Normally, nuclear reaction analysis involves irradiating a target with a high-energy ion that undergoes a nuclear reaction with an atom in the target, creating a different particle with an energy characteristic of the reaction. Thus, detecting the reaction product gives information about nuclear collisions between the primary ion and the target atoms. In our investigation, the incident ion does not undergo a nuclear reaction with an atom in the target, but transfers energy to an atom in the target (through any number of intermediate collisions), which then undergoes a nuclear reaction with another target atom. In this case, we can collect information about primary and higher-generation recoil atoms in the collision cascade. The number of reaction events detected can then be compared with predictions based on a model of the collision cascade.

We investigate the D(*d,p*)T fusion reaction in a target of titanium deuteride irradiated with Ar or Xe. The D(*d,p*)T reaction is well suited to this type of experiment because it produces relatively high-energy protons (3.02 MeV), which are easily detected and can escape from deep within the sample, and the cross section is large enough that fusion has been observed for incident deuteron energies as low as 3 keV (laboratory frame).⁴ Collision cascades resulting in D(*d,p*)T reactions will include collisions between two heavy atoms (Xe-Ti, Ar-Ti), a

heavy and a light atom (Xe-D, Ar-D, Ti-D), and two light atoms (D-D). Therefore, a model used to predict the fusion yield must adequately describe each type of interaction.

Titanium deuteride samples were prepared by evaporating 320 nm of Ti onto an oxidized silicon wafer. Pieces of the wafer were placed in a quartz tube, and the tube was mechanically pumped to 50 mTorr and filled with deuterium gas to a pressure of 16 psi above atmospheric pressure. The tube was heated to 420 °C for 30 min to dissolve the surface titanium oxide,⁵ and allow the deuterium to enter the Ti layer. The temperature was then lowered to 250 °C and the sample was annealed for 16 h to create a uniform TiD_{1.7} layer.

The deuterium content of the film was measured indirectly by 2 MeV He⁺⁺ backscattering spectrometry. By measuring the decrease in the height of the Ti signal due to the addition of deuterium, it was determined that the film was uniform with a stoichiometry of TiD_{1.7±0.2}. Backscattering also revealed the presence of a surface oxide 2–5 nm thick.

The titanium deuteride samples were irradiated with ion beams of 140, 150, 250, 300, 400, 450, and 500 keV Ar; and 200, 250, 300, and 500 keV Xe to doses ranging from 1.5 × 10¹⁶ to 4 × 10¹⁷ ions/cm². The beam currents ranged from 0.4 to 12.0 μA. During irradiation, the samples were kept at liquid-nitrogen temperature to minimize any radiation-enhanced diffusion or desorption of deuterium from the sample surface.

The ion beam was passed through a 1 cm square defining aperture onto a 1.2 × 1.2 cm titanium deuteride sample tilted 7° from the beam axis. A silicon surface barrier detector (25 mm² active area) was placed at an angle of 129° from the beam axis and 24 mm from the center of the sample. The detector was covered with a 1.35 mg/cm² (5 μm) aluminum absorber to block out any sputtered or backscattered particles. The detection system was calibrated using 5.477 MeV alpha particles from a ²³⁸Pu source, and 2.814, 2.614, 2.328, and 1.725 MeV alpha particles obtained by backscattering 3.05 MeV alpha particles [determined by ¹⁶O(*α,α*)¹⁶O resonance] from Au, Rh, Co, and Si samples, respectively, at an angle of 170°.

The ion dose was measured by integrating the ion current hitting the sample. The accuracy of the dose

measurement was checked by implanting the beam into a piece of Si immediately before and after the experiment. The ion dose in the Si was then measured using 2 MeV He^{++} backscattering spectrometry. The dose measured by charge integration was $5 \pm 3\%$ less than that measured by backscattering, and was corrected accordingly.

Spectra obtained during ion irradiation contain two broad peaks with roughly equal areas corresponding to 3.02 MeV protons and 1.01 MeV tritons from the $\text{D}(d,p)\text{T}$ nuclear reaction (Fig. 1). The peaks are shifted to lower energies by a few hundred keV due to the energy lost in the $5 \mu\text{m}$ Al absorber between the sample and the detector. The region between the peaks contains a uniform background that is probably due to high-energy protons that were scattered before entering the detector. This background scales linearly with the counts in the proton peak and is not present in background measurements with the beam off.

Background spectra were taken with $\text{TiD}_{1.7}$ samples and no beam, and with $\text{TiH}_{1.7}$ samples and a 250 keV Xe^+ beam, for 7–14 h. In both cases, the background was quite similar. The background count rate was 17 ± 3 counts per h, with almost all of the counts within the triton window (200–700 keV) and zero counts in the proton window (2.6–3.1 MeV). Typical fusion count rates were 100–4500 protons per h.

To determine the fusion yield, only the counts in the proton peak were considered in all irradiations because of the lesser background content of that peak. The total fusion yield (fusion reactions per incident ion) was calculated from the proton yield measured over the effective detector solid angle (43.7 mSr) by assuming that the angular distribution of reaction products is isotropic.⁶ The experimentally obtained fusion yields are listed in Table I. In some cases, the fusion yield decreased slightly with increasing dose, probably due to desorption of deuterium⁷ or dilution by the addition of the irradiating species. In those cases, only the initial fusion yield was retained for the interpretation.

A simple model, based on a linear binary collision cascade, can be used to estimate the fusion yield for a given ion-target combination. As the incident ion penetrates the target material, it transfers its energy to target atoms and electrons in nuclear and electronic collisions until it

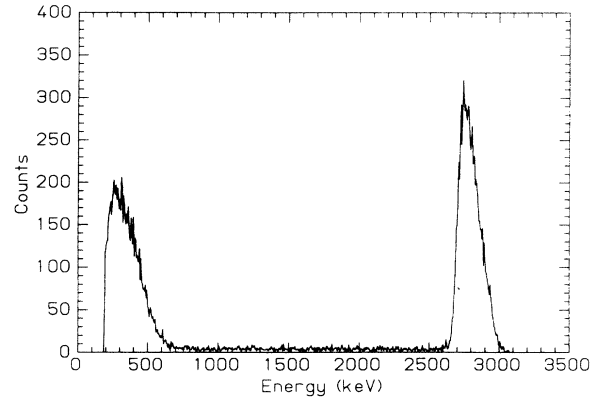


FIG. 1. Spectrum obtained by irradiating $\text{TiD}_{1.7}$ with 5.12×10^{16} 400 keV Ar^{++} ions over a duration of 2.0×10^4 s. The detector solid angle is 43.7 mSr. A $1.35 \mu\text{g}/\text{cm}^2$ Al absorber covering the detector lowers the detected energy of the proton and triton peaks.

comes to rest. For a fusion event to occur, energy must be transferred to a deuteron, which in the course of its displacement must strike a second deuteron and cause a fusion reaction. Given a deuteron with energy E_D (in the laboratory frame), the fusion yield, $Y_{\text{DD}}(E_D)$ is⁸

$$Y_{\text{DD}}(E_D) = \int_R^0 n_D \sigma_f(E_{\text{CM}}) dx \\ = \frac{n_D}{n_D + n_{\text{Ti}}} \int_0^{E_D} \frac{dE}{\varepsilon_D(E)} \sigma_f(E/2), \quad (1)$$

where x is the path length of the deuteron, R is its range, n_D and n_{Ti} are, respectively, the atomic densities of deuterons and titanium atoms in the target, ε_D is the sum of the nuclear and electronic stopping power of D in $\text{TiD}_{1.7}$ and σ_f is the fusion cross section for the center-of-mass energy $E_{\text{CM}} = E_{\text{lab}}/2$ for the reaction $\text{D}(d,p)\text{T}$.

There are many possible collision chains that can lead to the creation of an energetic deuteron. Each possible collision chain can be labeled by listing the atoms in the order of their involvement in the chain. Each chain resulting in a fusion reaction must begin with the incident ion and end with a deuteron striking a deuteron. Therefore, in the case of Xe irradiation of $\text{TiD}_{1.7}$, the simplest

TABLE I. Experimental and theoretical fusion yields.

Ion	Energy (keV)	Experimental yield (fusion events/ion)	Theoretical yield (fusion events/ion)
Ar	140	$(1.36 \pm 0.14) \times 10^{-12}$	1.38×10^{-12}
	150	$(1.77 \pm 0.18) \times 10^{-12}$	1.88×10^{-12}
	250	$(1.30 \pm 0.13) \times 10^{-11}$	1.40×10^{-11}
	300	$(3.04 \pm 0.30) \times 10^{-11}$	2.56×10^{-11}
	400	$(5.36 \pm 0.54) \times 10^{-11}$	5.95×10^{-11}
	450	$(8.16 \pm 0.82) \times 10^{-11}$	8.12×10^{-11}
	500	$(1.04 \pm 0.10) \times 10^{-10}$	1.06×10^{-10}
Xe	600	$(1.97 \pm 0.20) \times 10^{-10}$	1.61×10^{-10}
	200	$(8.48 \pm 1.30) \times 10^{-14}$	1.03×10^{-13}
	250	$(4.86 \pm 0.59) \times 10^{-13}$	4.22×10^{-13}
	300	$(1.28 \pm 0.13) \times 10^{-12}$	1.21×10^{-12}
	500	$(1.85 \pm 0.19) \times 10^{-11}$	1.56×10^{-11}

chain is Xe-D-D. More complicated chains include Xe-Ti-D-D, Xe-D-D-D, Xe-Ti-Ti-D-D, Xe-D-Ti-D-D, and so on. The total collision cascade caused by an incident ion can be broken down into a set of these chains. To obtain the total fusion yield for a cascade, the fusion yield contributed by each type of chain is calculated and these yields are summed.

$$Y_{\text{TiDD}}(E_{\text{Ti}}) = \frac{n_{\text{D}}}{n_{\text{D}} + n_{\text{Ti}}} \int_0^{E_{\text{Ti}}} \frac{dE}{\epsilon_{\text{Ti}}(E)} \int_0^{\gamma_{\text{Ti,D}}E} Y_{\text{DD}}(U) \frac{d\sigma(E, U_{\text{D}})}{dU_{\text{D}}} dU_{\text{D}}, \quad (2)$$

where $\gamma_{\text{Ti,D}} = 4M_{\text{Ti}}M_{\text{D}}/(M_{\text{Ti}} + M_{\text{D}})^2$ is the maximum energy transfer between Ti and D, and $d\sigma/dU_{\text{D}}$ is the differential scattering cross section for Ti-D collisions. This integral sums all possible Ti-D collisions during the slowing down of the Ti, weighted by the differential cross section. Next, the fusion yield $Y_{\text{TiTiDD}}(E)$ for the chain Ti-Ti-D-D is calculated using the general equation

$$Y_{a,b,\dots,\text{DD}}(E) = \frac{n_b}{n_{\text{D}} + n_{\text{Ti}}} \int_0^E \frac{dE_a}{\epsilon_a(E_a)} \int_0^{\gamma_{a,b}E_a} Y_{b,\dots,\text{DD}}(U_b) \frac{d\sigma(E_a, U_b)}{dU_b} dU_b, \quad (3)$$

where $a = \text{Ti}$, $b = \text{Ti}$, and $Y_{b,\dots,\text{DD}} = Y_{\text{TiDD}}$ [from Eq. (2)]. Finally, the incident ion is added to the chain and the fusion yield for the entire chain $Y_{\text{XeTiTiDD}}(E)$ is found using Eq. (3) with $a = \text{Xe}$, $b = \text{Ti}$, and $Y_{b,\dots,\text{DD}} = Y_{\text{TiTiDD}}$. All other chains are calculated in a similar manner.

The total fusion yield $Y_{\text{Xe}}(E)$ is found by summing the yields of the chains:

$$Y_{\text{Xe}}(E) = Y_{\text{XeDD}}(E) + Y_{\text{XeDDD}}(E) + Y_{\text{XeTiDD}}(E) + Y_{\text{XeTiTiDD}}(E) + \dots \quad (4)$$

However, since the energy of the penultimate deuteron in a chain decreases as the chain involves more intermediate steps, and the $\text{D}(d,p)\text{T}$ fusion cross section decreases extremely rapidly with decreasing energy, only the first few terms of Eq. (4) give significant contributions to $Y_{\text{Xe}}(E)$.

The fusion yield for each chain was calculated by numerical integration, with analytic expressions for the fusion cross section, stopping powers, and differential scattering cross section. The $\text{D}(d,p)\text{T}$ fusion cross section is given by⁶

$$\sigma_f(E) = \frac{S(E)}{E} e^{-b/E^{1/2}}, \quad (5)$$

where E is the center-of-mass energy, $b = 31.39 \text{ keV}^{1/2}$, and $S(E)$ is a polynomial fit to the astrophysical S factor given in Ref. 6. The nuclear and electronic stopping powers are calculated using the formulas in Ref. 9, except for the electronic stopping power of deuterons, which is taken from Ref. 10. The differential scattering cross section is of the form¹¹

$$\frac{d\sigma(E, U)}{dU} = \frac{\pi}{2} a^2 \lambda \frac{t^{-m}}{U} [1 + (2\lambda t^{1-m}q)^{-1/q}], \quad (6)$$

$$t = \frac{c_r^2}{\gamma} EU,$$

where a is the Firsov screening length, γ is the maximum

To calculate the yield for a given chain, one starts with the function $Y_{\text{DD}}(E_{\text{D}})$ from Eq. (1) and works backward through the chain to the incident ion. For example, for the chain Xe-Ti-Ti-D-D, the fusion yield for the chain segment Ti-D-D is calculated as a function of the initial energy of the Ti atom after being struck by the preceding Ti, using

fraction of energy transferable between the two atoms in the collision, c_r is the conversion factor from energy to the dimensionless "reduced" energy, and λ , m , and q are fitting parameters dependent on the type of interatomic potential assumed. We have used the values $\lambda = 1.70$, $m = 0.311$, and $q = 0.588$, corresponding to a Thomas-Fermi-Sommerfeld screened Coulomb potential.¹²

Calculations for 200–500 keV Xe irradiation show that the Xe-D-D chain contributes approximately 80% of the total fusion yield. The Xe-Ti-D-D chain contributes approximately 20%, and Xe-Ti-Ti-D-D contributes about 0.2% of the total yield. All others give less than 0.005%. For 140–600 keV Ar irradiation, the fusion yield is dominated by the Ar-D-D contribution. The Ar-Ti-D-D chain accounts for a little under 1% of the total yield, and all other chains combined contribute less than 0.01%.

The total fusion yield has been calculated for both Ar and Xe irradiation of titanium deuteride with a composi-

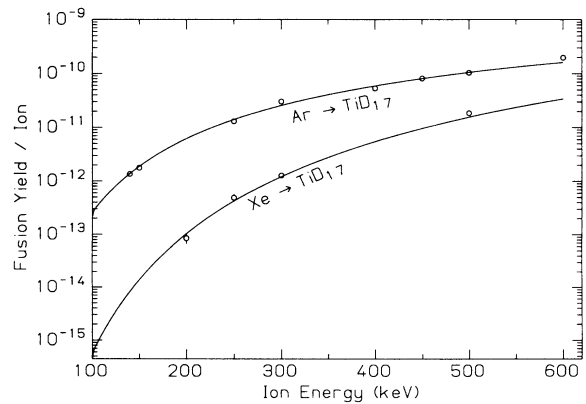


FIG. 2. Comparison of measured (circles) and calculated (lines) fusion yields for $\text{TiD}_{1.7}$ irradiated by Ar and Xe ions of various energies.

tion of $\text{TiD}_{1.7}$. In Fig. 2 and Table I, these calculated yields are compared to the experimentally obtained yields. The experimental yields correspond quite well to those calculated for both Ar and Xe irradiation.

These results show that the fusion yield of reactions produced by primary and higher-generation recoils generated by an incident ion can be quantitatively explained by a linear binary-collision cascade model. The rapid decrease in the $D(d,p)T$ cross section with decreasing energy limits the observable portion of the collision cascade to the first three generations of recoils. Within that limi-

tation, this experiment directly confirms the existence of a linear cascade as it unfolds with a solid.

The authors wish to acknowledge W. L. Johnson's participation in the conceptual phase of this experiment and in continued discussions. We thank C. A. Barnes for his guidance and many helpful discussions. The technical assistance by R. Gorris is gratefully appreciated. We also acknowledge the financial support by the National Science Foundation through MRG Grant No. DMR-8811795.

¹*Sputtering by Particle Bombardment I*, edited by R. Behrisch, Topics in Applied Physics Vol. 47 (Springer-Verlag, Berlin, 1981).

²T. D. Andreadis and J. Fine, Nucl. Instrum. Methods **209**, 495 (1983).

³O. Grizzi and R. A. Baragiola, Phys. Rev. A **35**, 135 (1987).

⁴J. Roth, R. Behrisch, W. Möller, and W. Ottenberger, Nucl. Fusion **30**, 441 (1990).

⁵T. Smith, Surf. Sci. **38**, 292 (1973).

⁶A. Krauss, H. W. Becker, H. P. Trautvetter, and C. Rolfs, Nucl. Phys. **A465**, 150 (1987).

⁷M. Schluckebier, Th. Pfeiffer, K. Muskalla, W. Schmülling, and D. Kamke, Appl. Phys. A **42**, 19 (1987).

⁸C. Carraro, B. Q. Chen, S. Schramm, and S. E. Koonin, Phys. Rev. A **42**, 1379 (1990).

⁹J. P. Biersack, E. Ernst, A. Monge, and S. Roth, *Tables of Electronic and Nuclear Stopping Powers and Energy Straggling for Low Energy Ions* (Hahn-Meitner-Institut, Berlin, 1975), pp. 3–5.

¹⁰H. H. Anderson and J. F. Ziegler, *Hydrogen Stopping Powers and Ranges in All Elements* (Pergamon, New York, 1977).

¹¹P. D. Townsend, J. C. Kelly, and N. E. W. Hartley, *Ion Implantation, Sputtering, and their Applications* (Academic, London, 1976), pp. 19–21.

¹²K. B. Winterbon, Radiat. Eff. **13**, 215 (1972).